# Photooxygenation of 1,1-Diarylethylenes via Addition of Oxygen to the 1,4-Dimer Radical Cations, Catalyzed by 10-Methylacridinium Ion

**Morifumi Fujita, Akira Shindo, Akito Ishida, Tetsuro Majima, Setsuo Takamuku,* and Shunichi Fukuzumi*,†**

The Institute of Scientific and Industrial Research, Osaka University, Ibaraki, Osaka 567

†Department of Applied Chemistry, Faculty of Engineering, Osaka University, Suita, Osaka 565

(Received September 27, 1995)

Photooxygenation of 1,1-diarylethylene occurs efficiently using 10-methylacridinium ion as a photocatalyst to yield the 1,2-dioxane and/or the diaryl ketone depending on the substituents on the aryl groups. The reaction mechanism is revealed based on the dependence of the quantum yields on the concentrations of the alkene and oxygen, the fluorescence quenching of 10-methylacridinium ion by the alkene, and the direct detection of reactive intermediates by applying laser flash spectroscopy as well as pulse radiolysis. The photooxygenation proceeds via photoinduced electron transfer from the alkene to the singlet excited state of 10-methylacridinium ion. The alkene radical cation formed by the photoinduced electron transfer reacts with alkene to give the 1,4-dimer radical cation, which then reacts with oxygen to produce the oxygenated 1,6-radical cation. The subsequent one-electron reduction of the 1,6-radical cation results in formation of the 1,6-biradical which cyclizes to yield 1,2-dioxane derivative or fragmentates to yield diaryl ketone. When the 1,6-biradical is reduced by the alkene itself, the alkene radical cation is regenerated to repeat the radical chain process.

There have been extensive studies on the photooxygenation of alkenes, using aromatic nitriles as photosensitizers.[1—9] Addition of oxygen to alkene radical cation is often proposed to be a key step.[3] However, aromatic nitriles known to function as triplet sensitizers produce singlet oxygen ($^1O_2$) that is a very reactive species.[4] The superoxide anion ($O_2^{-\bullet}$) may also be involved as an active oxygen species, since photoinduced electron transfer from substrates to the singlet excited states of nitriles is followed by facile electron transfer from the resulting radical anions to oxygen to produce $O_2^{-\bullet}$.[5] Thus, photooxygenation reactions so far studied may involve active oxygen species such as $^1O_2$ and $O_2^{-\bullet}$ rather than molecular oxygen.[4—6] On the other hand, 10-methylacridinium ion ($AcrH^+$) is known as an unique photosensitizer which produces neither $^1O_2$ nor $O_2^{-\bullet}$,[10,11] providing an excellent opportunity to gain comprehensive and confirmative understanding for the photocatalytic oxygenation mechanism.

We report herein the detailed mechanistic study on the photooxygenation of 1,1-diarylethylene (**1**) using $AcrH^+$ as a sensitizer. The reaction mechanism is revealed based on the dependence of the quantum yields on the concentrations of **1** and $O_2$, the fluorescence quenching of $AcrH^+$ by **1**, and the direct detection of reactive intermediates by applying laser flash spectroscopy as well as pulse radiolysis.

## Experimental

**Materials.** 10-Methylacridinium iodide was prepared by the reaction of acridine with methyl iodide in acetone, and it was converted to the perchlorate salt ($AcrH^+ClO_4^-$) by addition of magnesium perchlorate to the iodide salt, and purified by recrystallization from methanol. 1,1-Diphenylethylene (Tokyo Kasei Kogyo Co., Ltd.) was purified by column chromatography (alumina) before use. The other 1,1-diarylethylenes ($Ar^1Ar^2C{=}CH_2$: $Ar^1{=}Ar^2$=4-methoxyphenyl, $Ar^1$=4-methoxyphenyl, $Ar^2$=phenyl, and $Ar^1{=}Ar^2$=4-methylphenyl) were prepared by a Wittig reaction of corresponding $Ar^1COAr^2$ with $(C_6H_5)_3P{=}CH_2$ and purified by column chromatography (silica) and recrystallization from hexane. 3,3,6,6-Tetraaryl-1,2-dioxanes were isolated by filtration of white powder precipitated after photooxygenation of 1,1-diarylethylenes. Acetonitrile and 1,2-dichloroethane used as solvents were purified and dried by the standard procedure.

**Reaction Procedure.** A square quartz cuvette ($10\times10$ mm$^2$) which contained an MeCN solution (4.0 cm$^3$) of $AcrH^+$ ($1.7\times10^{-3}$ mol dm$^{-3}$) and 1,1-diarylethylene ($4\times10^{-3}$ mol dm$^{-3}$) was irradiated with monochromatized light of $\lambda = 366$ nm from an ultra high pressure mercury lamp (500 W). The photooxygenation was monitored by using a HPLC and UV-vis spectrophotometer. The photooxygenation products were identified by $^1$H NMR comparison with the literature.[8] The $^1$H NMR measurements were performed using Japan Electron Optics JNM-GSX-270 (270 MHz) NMR spectrometers.

**Quantum Yield Determinations.** A standard actinometer (potassium ferrioxalate) was used for the quantum yield determination of the photooxygenation of 1,1-diarylethylenes catalyzed by $AcrH^+$. A square quartz cuvette ($10\times10$ mm$^2$) which contained an MeCN solution (4.0 cm$^3$) of $AcrH^+$ ($1.7\times10^{-3}$ mol dm$^{-3}$) and 1,1-diarylethylene ($2.0\times10^{-3}$—$3.0\times10^{-2}$ mol dm$^{-3}$) was irradiated with monochromatized light of $\lambda = 366$ nm from an ultra high pressure mercury lamp (500 W) (the light intensity = $2.1\times10^{-8}$ einstein s$^{-1}$). Under the conditions of actinometry experiments, both the actinometer and $AcrH^+$ absorbed essentially all the inci-

dent light of $\lambda = 366$ nm. The photochemical reaction was monitored by HPLC. The quantum yields were determined from the increase in the concentration of oxygenated products per constant time. The oxygen concentration was controlled by bubbling with oxygen–nitrogen mixed gas and it was determined from oxygen partial pressure of introduced gas and solubility of oxygen into acetonitrile.

**Fluorescence Quenching.** Fluorescence measurements were performed on a Hitachi 850 spectrofluorophotometer. The excitation wavelength of $AcrH^+$ was chosen as 360 nm in MeCN. The monitoring wavelength was corresponding to the maximum of the emission band at 488 nm. Relative emission intensities were measured for an MeCN solution containing $AcrH^+$ ($5.0\times10^{-5}$ mol dm$^{-3}$) with 1,1-diarylethylene at various concentrations ($1\times10^{-3}$—$7\times10^{-3}$ mol dm$^{-3}$). There was no change in the shape but there was a change in the intensity of the fluorescence spectrum by the addition of 1,1-diarylethylene. The Stern–Volmer relationship (Eq. 1) was obtained for the ratio of the emission intensities in the absence and presence of 1,1-diarylethylene ($I_0/I$) vs. the concentration of 1,1-diarylethylene ([D]). The observed quenching rate constants $k_q$ ($=K_{SV}\tau^{-1}$) were obtained from the Stern–Volmer constants $K_{SV}$ and the fluorescence lifetime ($\tau = 37$ ns)[10] of $AcrH^+$.

$$I_0/I = 1 + K_{SV}[D]. \quad (1)$$

**Laser-Flash Photolysis.** The sample solution is introduced into a $10\times10$ mm$^2$ quartz cell. Nd : YAG laser (third harmonic, 355 nm; 4-ns pulse width; 180 mJ/pulse) was used for sample excitation. The excitation light was parallel to the analyzing light from a 450-W xenon lamp (Osram, XBO-450). The analyzing light passing through a sample cell was focused to a computer-controlled monochromator (CVI Digikrom-240) by two lenses and four mirrors. The output light of monochromator was monitored by a photomultiplier tube (PMT; Hamamatsu Photonix, R1417). The signal from a PMT was recorded on a transient digitizer (Tektronix, 7912AD with plug-ins, 7A19 and 7B92A). Total system control and data processing were carried out with a microcomputer (Sharp, X-6800) which was connected to the measurement components with a GP-IB interface.

**Pulse Radiolysis.** The L-band linear accelerator at Osaka University was used as the source of electron pulse. The energy was 28 MeV and the pulse width was 8 ns. The peak current was 8 A and the dose was 0.7 kGy per pulse. The diameter of the electron beam spot on the surface of a cell was ca. 4 mm. A 450-W xenon lamp (Osram, OPG-450) was used as the analyzing light source. The light passing through a sample solution was monitored by a photomultiplier (Hamamatsu Photonics, R-928) after a monochromator (Nikon, G-250). The light signal was developed on a transient digitizer (Tektronix, 7912AD). A spectral grade of 1,2-dichloroethane was used as a solvent. The sample solutions were filled in a Suplasil quartz cell ($10\times10$ mm$^2$).

**Electrochemical Measurements.** The second harmonic ac voltammetry (SHACV) measurements of 1,1-diarylethylenes were carried out with a BAS 100B electrochemical analyzer in a deaerated MeCN solution containing 0.10 mol dm$^{-3}$ $NBu^n{}_4ClO_4$ as a supporting electrolyte at 298 K. The platinum working electrode (BAS) was polished with BAS polishing alumina suspension and rinsed with acetone before use. The counter electrode was platinum wire (BAS). The measured potentials were recorded with respect to an $Ag/AgNO_3$ ($1.0\times10^{-2}$ mol dm$^{-3}$) reference electrode. The $E^\circ{}_{ox}$ values (vs. $Ag/Ag^+$) are converted into those vs. SCE by addition of 0.29 V.[12]

## Results and Discussion

**Photooxygenation of 1,1-Diarylethylene, Catalyzed by 10-Methylacridinium Ion.** Visible light irradiation of the absorption band ($\lambda_{max}$=358 nm) of 10-methylacridinium perchlorate ($AcrH^+ ClO_4^-$ : $1.7\times10^{-3}$ mol dm$^{-3}$) in an oxygen-saturated acetonitrile (MeCN) solution containing 1,1-diarylethylene (**1**) ($4.0\times10^{-3}$ mol dm$^{-3}$) gave 3,3,6,6-tetraaryl-1,2-dioxane (**2**) and diaryl ketone (**3**) (Eq. 2) depending on the substrate **1a**—**d** as shown in Table 1. Oxygenation of **1a** and **1b** yields exclusively dioxane (**2a** and **2b**), respectively. In the case of **1c**, however, both dioxane (**2c**) and ketone (**3c**) are obtained, while in the case of **1d**, only ketone (**3d**) is obtained without formation of dioxane (**2d**). During the reaction, the concentration of $AcrH^+$ remains constant, indicating that $AcrH^+$ acts as an efficient photocatalyst for the photooxygenation of **1**.

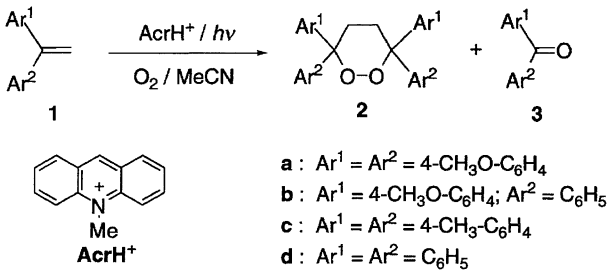


(2)

**Laser Flash Photolysis and Pulse Radiolysis.** Laser flash irradiation (355 nm from a Nd : YAG laser) of **1a** ($1.3\times10^{-2}$ mol dm$^{-3}$) in a deaerated MeCN solution containing $AcrH^+$ ($5.0\times10^{-5}$ mol dm$^{-3}$) gave transient absorption spectra which consist of superposition of the absorption bands due to the dimer radical cation of **1a** (**4a**: $\lambda_{max}$=340, 490 nm)[13] and 10-methylacridinyl radical ($AcrH^\bullet$: a broad absorption band between 450 and 540 nm).[14] The results are shown in Fig. 1 which indicates that photoinduced electron transfer from **1a** to $AcrH^+$ occurs to yield radical cation of **1a** ($\mathbf{1a}^{+\bullet}$) as well as $AcrH^\bullet$, and that $\mathbf{1a}^{+\bullet}$ reacts rapidly with **1a** to give the dimer radical cation (**4a**).[13] In the presence of oxygen under otherwise the same conditions, the transient absorption due to **4a** decays rapidly, accompanied by concomitant appearance of new absorption band at 500 nm as also shown in Fig. 1. The new absorption band agrees with the reported band due to the oxygenated 1,6-radical cation

Table 1. Photooxygenation of 1,1-Diarylethylene (**1**) ($4\times10^{-3}$ mol dm$^{-3}$) with Oxygen, Catalyzed by $AcrH^+$ ($1.7\times10^{-3}$ mol dm$^{-3}$) in Oxygen-Saturated MeCN

| | Time | Conversion | Yield/%[a] | |
|---|---|---|---|---|
| **1** | min | % | **2** | **3** |
| **a** | 30 | 85 | 100 | 0 |
| **b** | 30 | 80 | 100 | 0 |
| **c** | 50 | 70 | 60 | 40 |
| **d** | 90 | 70 | 0 | 80 |

a) HPLC yield based on the conversion yield of **1**.

(**5a**) which may be formed by addition of oxygen to **4a**.[13]

Although the transient spectrum of AcrH• is significantly overlapped with that of **4a** in Fig. 1, the transient spectrum of the dimer radical cation (**4c**) is slightly blue-shifted as compared to that of **4a**, and thereby it is separated from that of AcrH• as shown in Fig. 2.[15,16] In order to confirm the formation of **4c**, the pulse radiolysis of **1c** ($1.0\times10^{-2}$ mol dm$^{-3}$) was performed in 1,2-dichloroethane (DCE) to produce **4c** by a similar manner to the case reported for **4a**.[13]

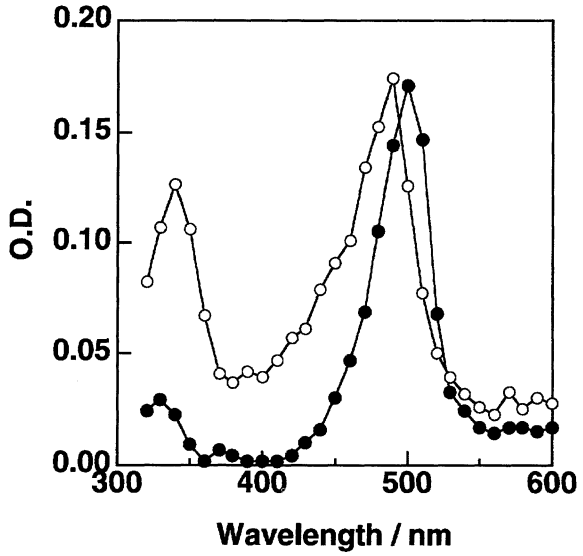


Fig. 1. Transient absorption spectra observed in laser-flash photolysis of **1a** ($1.3\times10^{-2}$ mol dm$^{-3}$) in deaerated (○) and aerated (●) MeCN containing AcrH$^+$ ($5\times10^{-5}$ mol dm$^{-3}$). Spectra were recorded in 0.5 μs (○) and 6 μs (●) after the laser pulse.

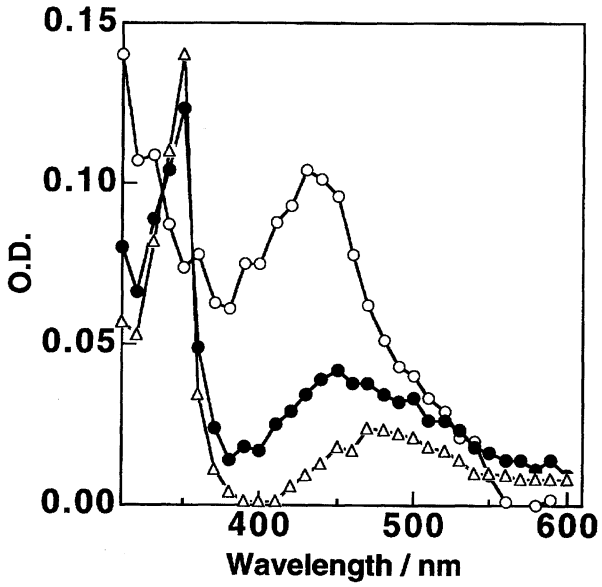


Fig. 2. Transient absorption spectra observed in laser-flash photolysis of **1c** ($1.3\times10^{-2}$ mol dm$^{-3}$) in deaerated MeCN containing AcrH$^+$ ($5.0\times10^{-5}$ mol dm$^{-3}$). Spectra were recorded in 0.5 μs (○), 3 μs (●), and 11 μs (△) after the laser pulse.

The transient spectrum of **4c** ($\lambda_{max}$=420 nm) is shown in Fig. 3, agreeing with that observed in Fig. 2.[17] In Fig. 3, an increase in absorbance at 370 nm is seen immediately after the pulse (10 ns), while the absorbance at 420 nm increases within several tens ns after the pulse to reach a maximum depending on the concentration of **1c**. Such a change in the transient spectra is ascribed to the dimer formation process from **1c**$^{+\bullet}$ to **4c** as observed in the case of **1a**.[13] Similarly the transient absorption spectra of the dimer radical cation of **1b** and **1d** (**4b**: $\lambda_{max}$=440 nm, **4d**: $\lambda_{max}$=400 nm) were observed in laser flash photolysis of a deaerated MeCN solution containing AcrH$^+$ and **1b** as well as **1d**. The transient absorption spectra of **1b** and **1d** agreed with those observed in the pulse radiolysis in DCE. In the presence of oxygen, the transient absorption bands due to **1b** and **1c** disappeared rapidly, accompanied by formation of **5b** ($\lambda_{max}$=550 nm) and **5c** ($\lambda_{max}$=560 nm), respectively.

The second-order rate constant for formation of the 1,4-dimer radical cation **4a** was determined as $5\times10^9$ dm$^3$ mol$^{-1}$ s$^{-1}$ from the rates of appearance of the absorption band due to **4a** at various concentrations of **1a**. The second-order rate constant for addition of oxygen to **4a** was also determined as $1\times10^9$ dm$^3$ mol$^{-1}$ s$^{-1}$ from the rates of disappearance of the absorption band due to **4a** in the presence of oxygen.

**Fluorescence Quenching.** Irradiation of the absorption band of AcrH$^+$ causes fluorescence at 488 nm in both deaerated and aerated MeCN. The fluorescence of $^1$AcrH$^{+*}$ is hardly quenched by molecular oxygen, but it is quenched efficiently by 1,1-diarylethylenes (**1**). The quenching rate constants $k_q$ are determined from the slopes of the Stern–Volmer plots and the life time of the singlet excited state $^1$AcrH$^{+*}$ ($\tau$=37 ns).[10] The $k_q$ values thus determined are listed in Table 2, where the $k_q$ values are close to the diffusion limited value ($2.0\times10^{10}$ dm$^3$ mol$^{-1}$ s$^{-1}$)[10] and they agree well with

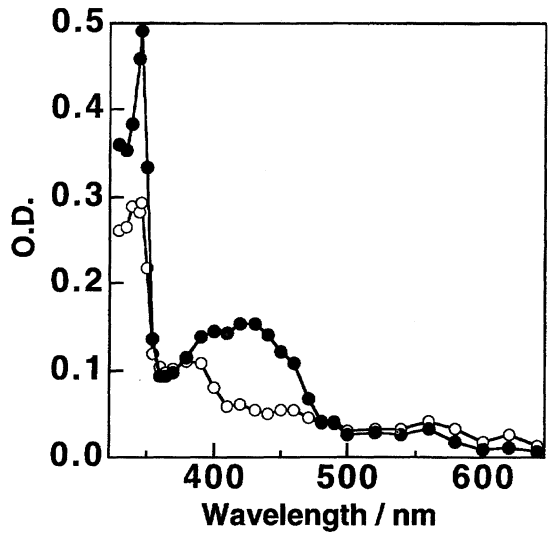


Fig. 3. Transient absorption spectra observed in pulse radiolysis of **1c** ($1.0\times10^{-2}$ mol dm$^{-3}$) in deaerated DCE. Spectra were recorded in 10 ns (○) and 40 ns (●) after the electron pulse.

those in the presence of oxygen. The one-electron oxidation potentials ($E^{\circ}_{ox}$) of 1,1-diarylethylenes **1** (1.44—1.94 V vs. SCE)[18] in Table 2 are much more negative than the reduction potential of $^1AcrH^{+*}$ (2.32 V vs. SCE),[10] and thereby the free energy change of electron transfer from **1** to $^1AcrH^{+*}$ is largely negative as listed in Table 2. Thus, the fluorescence quenching of $^1AcrH^{+*}$ by **1** may occur via electron transfer from **1** to $^1AcrH^{+*}$ at the diffusion-controlled rate as shown in Table 2.

**Quantum Yield.** The quantum yield ($\Phi$) of the photooxygenation of **1a** to dioxane (**2a**) under irradiation of light of $\lambda$ =366 nm increases linearly with an increase in the concentration of **1a** to exceed unity e.g.; $\Phi$=2 in $O_2$-saturated MeCN containing $1.5\times10^{-2}$ mol dm$^{-3}$ of **1a**) as shown in Fig. 4. Such large quantum yields suggest that the photooxygenation of **1a** proceeds via a photoinduced chain process. The $\Phi$ value increases also with an increase in the concentration of $O_2$ at a constant concentration of **1a** as shown in Fig. 5. In the case of **1c**, which is oxidized to **2c** and **3c**, the $\Phi$ values for formation of **2c** and **3c** increase in a parallel manner to each other with an increase in the concentration of **1c** as shown in Fig. 6, where the sum of both $\Phi$ values exceed unity at the high concentrations of **1c**. The large $\Phi$ values exceeding unity were also obtained in the photooxygenation of **1b** to **2b**. Thus, the photooxygenation of not only **1a** but also **1b** and **1c** may proceed via a chain process.

In contrast with the case of **1a**—**c**, the $\Phi$ value for photooxygenation of **1d** to benzophenone **3d** increases with an increase in the concentration of **1d**, but it approaches a limiting value at the high concentrations as shown in Fig. 7. Thus, the photooxygenation of **1d** may proceed via a nonchain process rather than a chain process. In this case, the $\Phi$ value remains constant with an increase in the concentration

Table 2. Rate Constants ($k_q$) for Fluorescence Quenching of $^1AcrH^{+*}$ by 1,1-Diarylethylene (**1**), One-Electron Oxidation Potentials ($E^{\circ}_{ox}$) of **1**, and Free Energy Change ($\Delta G^{\circ}_{et}$) of Photoinduced Electron Transfer from **1** to $^1AcrH^{+*}$ in MeCN

| 1 | $k_q$ / dm$^3$ mol$^{-1}$ s$^{-1}$ | $E^{\circ}_{ox}$ [a] / V vs. SCE | $\Delta G^{\circ}_{et}$ [b] / kcal mol$^{-1}$ |
|---|---|---|---|
| **a** | $1.0\times10^{10}$ | 1.44 (1.32) | −20 (−23) |
| **b** | $1.5\times10^{10}$ | 1.54 (1.39) | −18 (−21) |
| **c** | $1.5\times10^{10}$ | c) (1.66) | c) (−15) |
| **d** | $1.3\times10^{10}$ | 1.97 (1.88) | −8 (−10) |

a) Data in parentheses are irreversible potentials reported in Ref. 8. b) Values in parentheses are calculated from the irreversible potentials. c) Not determined.

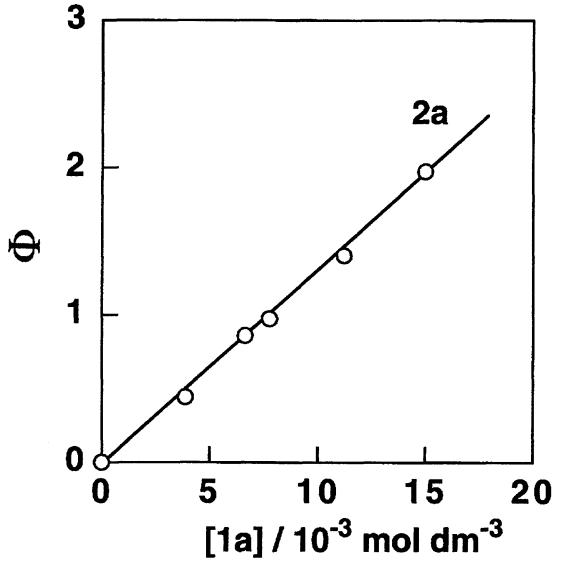


Fig. 4. Plot of the quantum yield ($\Phi$) vs. the concentration of **1a** for the photooxygenation of **1a** to **2a**, catalyzed by $AcrH^+$ ($1.7\times10^{-3}$ mol dm$^{-3}$) in $O_2$-saturated MeCN.

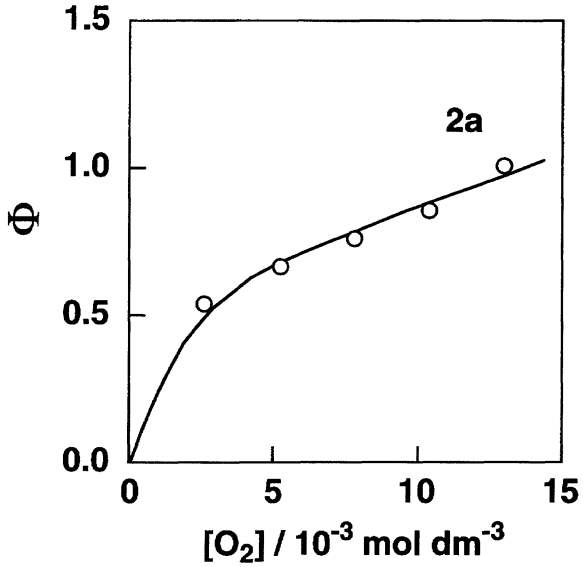


Fig. 5. Plot of the quantum yield ($\Phi$) vs. the concentration of $O_2$ for the photooxygenation of **1a** ($8.2\times10^{-3}$ mol dm$^{-3}$) to **2a**, catalyzed by $AcrH^+$ ($1.7\times10^{-3}$ mol dm$^{-3}$) in MeCN.

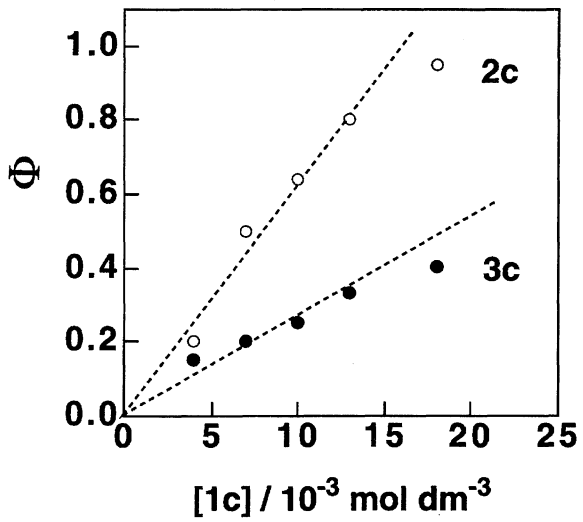


Fig. 6. Plots of the quantum yield ($\Phi$) vs. the concentration of **1c** for the photooxygenation of **1c** to **2c** (○) and **3c** (●), catalyzed by $AcrH^+$ ($1.7\times10^{-3}$ mol dm$^{-3}$) in $O_2$-saturated MeCN.

of $O_2$ as shown in Fig. 8.

**Photooxygenation Mechanism.** All the experimental results described above can be well explained by a single reaction mechanism in which the photooxygenation occurs via photoinduced electron transfer from **1** to $^1AcrH^{+*}$ as shown in Scheme 1. The photoinduced electron transfer gives radical cation of **1** ($\mathbf{1}^{+\bullet}$) and 10-methylacridinyl radical ($AcrH^\bullet$). The radical cation $\mathbf{1}^{+\bullet}$ immediately adds to **1** to produce the 1,4-dimer radical cation **4** ($k_1$) in competition with the back electron transfer to the reactant pair ($k_2$). The formation of both $AcrH^\bullet$ and **4** has been confirmed as shown in Figs. 1 and 2. Since the cationic and radical sites are separated from each other in **4**, the addition of triplet oxygen may occur efficiently to form the oxygenated 1,6-radical cation (**5**) ($k_3$) in competition with the back electron transfer to the reactants ($k_4$). The decrease in **4** accompanied by the formation of **5** has also been confirmed as shown in Fig. 1. The oxygenated 1,6-radical cation **5** may be reduced to the dioxane (**2**) or the ketone (**3**) and HCHO by **1** to give the 1,6-biradical **6**, accompanied by regeneration of $\mathbf{1}^{+\bullet}$ which starts the radical chain process again ($k_5$). The back electron transfer from $AcrH^\bullet$ to **5** ($k_6$) may also result in formation of the products **2** or **3** and HCHO. In the case of photooxygenation of **1c**, the dependence of the quantum yields for formation of **2c** on the concentrations of **1c** is in parallel with that of **3c** as shown in Fig. 6. Such a parallel dependence indicates the existence of a common intermediate for the formation of both products. Thus, not only **2c** but also **3c** may be formed from fragmentation of 1,6-biradical **6c** as shown in Scheme 1. The dioxane formation is favored as compared to the ketone formation by substituents of enhanced electron-donating properties (Table 1) as reported previously.[8]

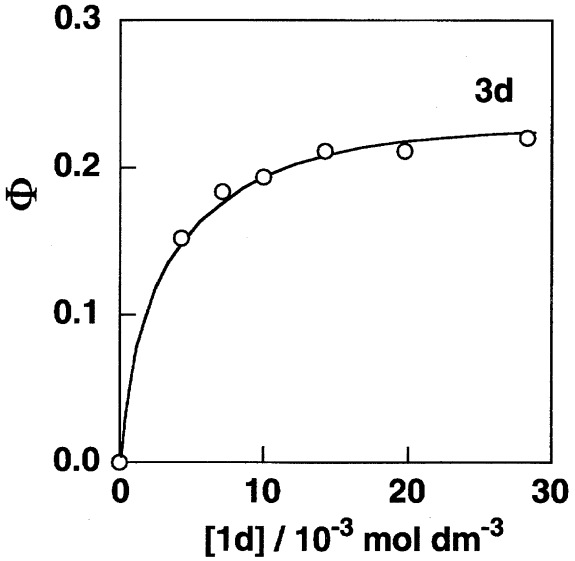


Fig. 7. Plot of the quantum yield ($\Phi$) vs. the concentration of **1d** for the photooxygenation of **1d** to **3d**, catalyzed by $AcrH^+$ ($1.7\times10^{-3}$ mol dm$^{-3}$) in $O_2$-saturated MeCN.

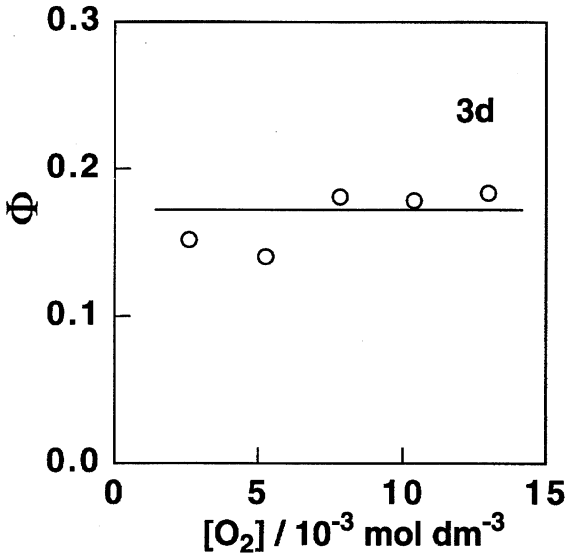


Fig. 8. Plot of the quantum yield ($\Phi$) vs. the concentration of $O_2$ for the photooxygenation of **1d** ($8.2\times10^{-3}$ mol dm$^{-3}$) to **3d**, catalyzed by $AcrH^+$ ($1.7\times10^{-3}$ mol dm$^{-3}$) in MeCN.

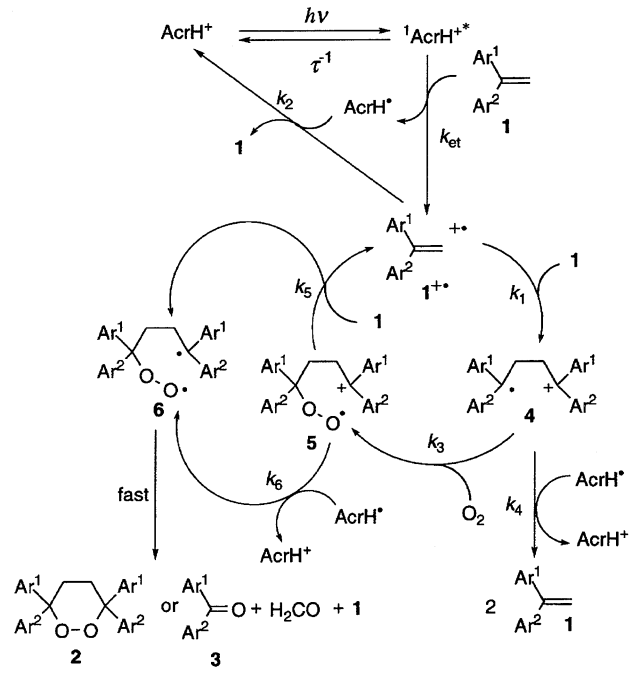


Scheme 1.

According to Scheme 1, the rates of various species involved in the photooxygenation reaction are given by Eqs. 3, 4, 5, 6, and 7, where $I_a$ is the light intensity absorbed by $AcrH^+$, and all the rate constants are defined in Scheme 1.

$$d[^1AcrH^{+*}]/dt = I_a - k_{et}[\mathbf{1}][^1AcrH^{+*}] - \tau^{-1}[^1AcrH^{+*}], \quad (3)$$

$$d[\mathbf{1}^{+\bullet}]/dt = k_{et}[\mathbf{1}][^1AcrH^{+*}] - k_1[\mathbf{1}^{+\bullet}][\mathbf{1}] + k_5[\mathbf{5}][\mathbf{1}] - k_2[\mathbf{1}^{+\bullet}][AcrH^\bullet], \quad (4)$$

$$d[\mathbf{4}]/dt = k_1[\mathbf{1}^{+\bullet}][\mathbf{1}] - k_3[\mathbf{4}][O_2] - k_4[\mathbf{4}][AcrH^\bullet], \quad (5)$$

$$d[\mathbf{5}]/dt = k_3[\mathbf{4}][O_2] - k_5[\mathbf{5}][\mathbf{1}] - k_6[\mathbf{5}][AcrH^\bullet], \quad (6)$$

$$d[AcrH^{\bullet}]/dt = k_{et}[\mathbf{1}][{}^{1}AcrH^{+*}] - k_2[\mathbf{1}^{+\bullet}][AcrH^{\bullet}] - k_4[\mathbf{4}][AcrH^{\bullet}] - k_6[\mathbf{5}][AcrH^{\bullet}]. \quad (7)$$

By applying the steady-state approximation to the reactive species $^{1}AcrH^{+*}$, $\mathbf{1}^{+\bullet}$, **4**, **5**, and $AcrH^{\bullet}$ in Eqs. 3, 4, 5, 6, and 7, the dependence of $\Phi$ on [**1**] and $[O_2]$ can be derived as given by Eqs. 8, 9, and 10.[19] The observation of **5a** in the

$$\Phi = k_{et}\tau[\mathbf{1}]k_6/\alpha(1+k_{et}\tau[\mathbf{1}]) + [k_{et}\tau[\mathbf{1}]/(1+k_{et}\tau[\mathbf{1}])\alpha\beta I_a]^{1/2}, \quad (8)$$

$$\alpha = k_6 + (k_2k_5/k_1) + k_4k_5[\mathbf{1}]/(k_3[O_2]), \quad (9)$$

$$\beta = 1 + k_5/k_1 + k_5[\mathbf{1}]/(k_3[O_2]). \quad (10)$$

laser flash photolysis (Fig. 1) indicates that the rate of the reaction of **5a** with **1** is much slower than those of the reaction of $\mathbf{1a}^{+\bullet}$ with **1a** and the reaction of **4a** with $O_2$, i.e., $k_5/k_1$, $k_5[\mathbf{1a}]/(k_3[O_2]) \ll 1$, when $\beta$ in Eq. 10 is reduced to $\beta \cong 1$. The back electron transfer reactions from $AcrH^{\bullet}$ to $\mathbf{1}^{+\bullet}$ ($k_2$) and **4** ($k_4$) may be highly exergonic process judging from the one-electron redox potentials (Table 2) and thereby the rate constants may be close to the diffusion rate constant ($2.0\times10^{10}$ $dm^3\,mol^{-1}\,s^{-1}$).[10] On the other hand, the rate constant of the reaction of **4** with $O_2$ ($k_1 = 1\times10^{9}$ $dm^3\,mol^{-1}\,s^{-1}$) is only one-fifth of that of formation of **4** ($k_3 = 5\times10^{9}$ $dm^3\,mol^{-1}\,s^{-1}$), vide supra. In such a case, Eq. 8 would be reduced to Eq. 11, provided that the $k_6$ value is much slow than the $k_5$ value ($k_6 \ll k_5$).[20]

$$\Phi = k_5[\mathbf{1}][k_3k_{et}\tau[O_2]/(1+k_{et}\tau[\mathbf{1}])k_4k_5I_a]^{1/2}. \quad (11)$$

According to Eq. 11, $\Phi$ should increase with an increase in [**1**] to exhibit the first-order dependence on [**1**] at low concentrations of **1**, changing to the one-half-order dependence on [**1**] at higher concentrations of **1**. Such a dependence of $\Phi$ on [**1**] is indeed observed in Fig. 6, where $\Phi$ is proportional to [**1a**—**c**] but deviation from the linear correlation (the broken line) to the lower values is observed at the high concentrations due to the gradual change from the first-order dependence on [**1a**—**c**] to the one-half-order dependence. The dependence of $\Phi$ on $[O_2]$ also agrees with that expected from Eq. 11 in which $\Phi$ is proportional to $[O_2]^{1/2}$. This is shown as a linear plot of $\Phi^2$ vs. $[O_2]$ in Fig. 9, where the data in Fig. 5 are replotted.[21]

In the case of **1d**, the $\Phi$ values become constant at the high concentrations of **1d**, indicating no involvement of radical chain processes in Scheme 1. Judging from the high oxidation potential of **1d** as compared to those of **1a**—**c** in Table 2, it is likely that electron transfer from $AcrH^{\bullet}$ to **5d** ($k_6$) is much faster than that to **5a**—**c**. In such a case, electron transfer from **1** to **5d** to regenerate $\mathbf{1d}^{+\bullet}$ ($k_5$) may be prevented by the fast electron transfer from $AcrH^{\bullet}$ to **5d**, which corresponds to the fast termination step ($k_6$) of the radical chain process, when the photooxygenation of **1d** may proceed via a non-chain pathway. The dependence of $\Phi$ on [**1**] in Eq. 6 is then reduced to Eq. 12, which is rewritten by Eq. 13, where $\Phi_\infty = 1 + k_2k_5/k_1k_6$. A linear plot of

$$\Phi = k_{et}\tau[\mathbf{1d}](1+k_2k_5/k_1k_6)/(1+k_{et}\tau[\mathbf{1d}]), \quad (12)$$

$$\Phi^{-1} = \Phi_\infty{}^{-1}[1 + (k_{et}\tau[\mathbf{1d}])^{-1}]. \quad (13)$$

$\Phi^{-1}$ and $[\mathbf{1d}]^{-1}$ is shown in Fig. 10, where the data in Fig. 7 are replotted. The $\Phi_\infty$ and $k_{et}$ values are obtained from the slope and intercept of the linear plot of $\Phi^{-1}$ vs. $[\mathbf{1d}]^{-1}$ as 0.24 and $1.2\times10^{10}$ $dm^3\,mol^{-1}\,s^{-1}$, respectively. The $k_{et}$ value agrees well with that obtained independently from the fluorescence quenching of $^{1}AcrH^{+*}$ by **1d** in Table 2 ($1.3\times10^{10}$ $dm^3\,mol^{-1}\,s^{-1}$). Such an agreement indicates strongly that the photooxygenation of **1d** proceeds via photoinduced electron transfer from **1d** to $^{1}AcrH^{+*}$ as shown in Scheme 1 where the chain propagation step ($k_5$) is stopped by the facile termination step ($k_6$) in the case of **1d** to yield

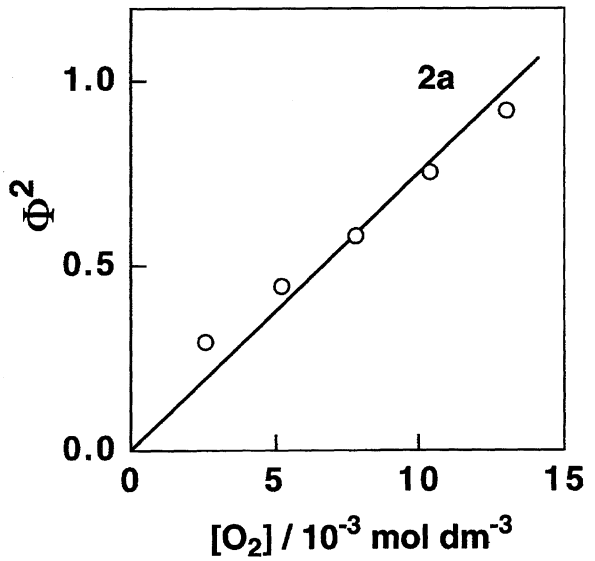


Fig. 9. Plot of $\Phi^2$ vs. the concentration of $O_2$ for the photooxygenation of **1a** ($8.2\times10^{-3}$ mol $dm^{-3}$) to **2a**, catalyzed by $AcrH^{+}$ ($1.7\times10^{-3}$ mol $dm^{-3}$) in MeCN.

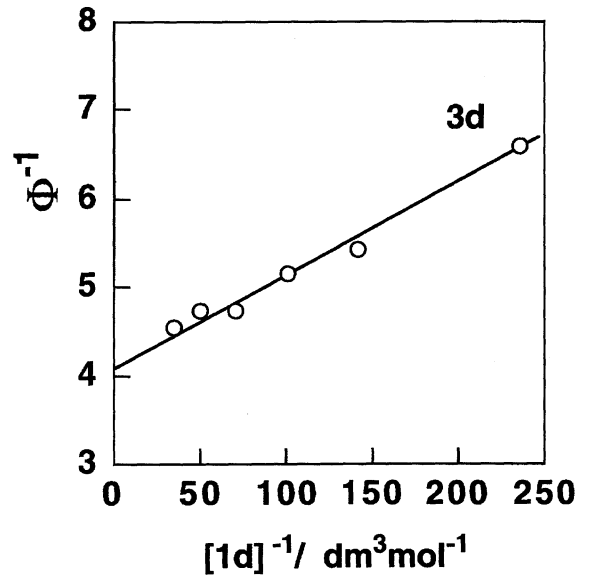


Fig. 10. Plot of $\Phi^{-1}$ vs. $[\mathbf{1d}]^{-1}$ for the photooxygenation of **1d** to **3d**, catalyzed by $AcrH^{+}$ ($1.7\times10^{-3}$ mol $dm^{-3}$) in $O_2$-saturated MeCN.

**3d**.

In conclusion, $AcrH^+$-catalyzed photooxygenation of **1** proceeds via addition of oxygen to dimer radical cation **4** to produce **5**, followed by the one-electron reduction of **5** to yield 1,6-biradical (**6**), which cyclizes to **2** or fragmentates to **1** and **3** depending on the substrate **1a—d**. When **5** is reduced mainly by **1** instead of $AcrH^•$ which is produced in the initial photoinduced electron transfer from **1** to $^1AcrH^{+*}$, $\mathbf{1}^{+•}$ is regenerated to repeat the chain process. When back electron transfer from $AcrH^•$ to **5** is much faster than electron transfer from **1** to **5** as is the case of **1d**, no radical chain process may be involved in the photooxygenation.

This work was partly supported by a Grant-in-Aid No. 0545312 from the Ministry of Education, Science and Culture. We thank Fellowships of the Japan Society for the Promotion of Science for Japanese Junior Scientists for financial support.

## References

1) M. Chanon, M. Julliard, J. Santamaria, and F. Chanon, *Nouv. J. Chim.*, **16**, 171 (1992); S. F. Nelsen, *Acc. Chem. Res.*, **20**, 269 (1987).

2) K. Mizuno and Y. Otsuji, "Topics in Current Chemistry," ed by J. Mattay, Springer-Verlag, Berlin (1994), Vol. 169, pp. 301—346; K. Yamaguchi, K. Takada, Y. Otsuji, and K. Mizuno, "Organic Peroxides," ed by W. Ando, John Wiley & Sons Ltd., New York (1992), pp. 1—100.

3) R. Akaba, K. Ohshima, Y. Kawai, Y. Obuchi, A. Negishi, H. Sakuragi, and K. Tokumaru, *Tetrahedron Lett.*, **32**, 109 (1991); R. Akaba, H. Sakuragi, and K. Tokumaru, *J. Chem. Soc., Perkin Trans. 2*, **1991**, 291; S. F. Nelsen and R. Akaba, *J. Am. Chem. Soc.*, **103**, 2096 (1981).

4) J. Santamaria, "Photoinduced Electron Transfer," ed by M. A. Fox and M. Chanon, Elsevier, Amsterdam (1988), Part B, Chap. 3, p. 483; D. C. Dobrowolski, P. R. Ogilby, and C. S. Foote, *J. Phys. Chem.*, **87**, 2261 (1983); J. Santamaria and R. Ouchabane, *Tetrahedron*, **42**, 5559 (1986).

5) K. Gollnick and A. Schnatterer, *Tetrahedron Lett.*, **25**, 185 (1984); K. Gollnick and A. Schnatterer, *Tetrahedron Lett.*, **25**, 2735 (1984); J. Eriksen and C. S. Foote, *J. Am. Chem. Soc.*, **102**, 6083 (1980).

6) K. Gollnick and S. Held, *J. Photochem. Photobiol. A: Chem.*, **59**, 55 (1991); K. Gollnick and S. Held, *J. Photochem. Photobiol. A: Chem.*, **70**, 135 (1993).

7) S. L. Mattes and S. Farid, *J. Am. Chem. Soc.*, **108**, 7356 (1986).

8) K. Gollnick, A. Schnatterer, and G. Utschick, *J. Org. Chem.*, **58**, 6049 (1993).

9) a) K. Mizuno, T. Tamai, I. Hashida, Y. Otsuji, Y. Kuriyama, and K. Tokumaru, *J. Org. Chem.*, **59**, 7329 (1993); b) T. Tamai, K. Mizuno, I. Hashida, Y. Otsuji, A. Ishida, and S. Takamuku, *Chem. Lett.*, **1994**, 149.

10) a) S. Fukuzumi and T. Tanaka, "Photoinduced Electron Transfer," ed by M. A. Fox and M. Chanon, Elsevier, Amsterdam (1988), Part C, pp. 578—635; b) S. Fukuzumi, "Advances in Electron Transfer Chemistry," ed by P. S. Mariano, JAI Press, Greenwich (1992), Vol. 2, pp. 67—175; c) M. Fujita and S. Fukuzumi, *J. Mol. Catal.*, **90**, L225 (1994).

11) K. Kikuchi, C. Sato, M. Watabe, H. Ikeda, Y. Takahashi, and T. Miyashi, *J. Am. Chem. Soc.*, **115**, 5180 (1993).

12) C. K. Mann and K. K. Barnes, "Electrochemical Reactions in Nonaqueous Systems," Marcel Dekker, New York (1970).

13) M. Kojima, A. Ishida, and S. Takamuku, *Chem. Lett.*, **1993**, 979.

14) K. S. Peters, E. Pang, and J. Rudzki, *J. Am. Chem. Soc.*, **104**, 5535 (1982); A. T. Poulos, G. S. Hammond, and M. E. Burton, *Photochem. Photobiol.*, **34**, 169 (1981).

15) As seen in Fig. 2, the absorption band due to **4c** ($\lambda_{max}$=430 nm) disappears in 11 μs after the laser pulse, when the band due to $AcrH^•$ around 500 nm remains because of the difference in their stability.

16) Similar blue-shifts have been reported for diarylmethyl cations with less electron donating substituents; R. A. McClelland, V. M. Kanagasabapathy, and S. Steenken, *J. Am. Chem. Soc.*, **110**, 6913 (1988).

17) The absorption band at 350 nm due to **4c** in Fig. 3 is not observed clearly in the laser flash photolysis of the **1c**–$AcrH^+$ system in Fig. 2 because of the bleaching of the absorption band of $AcrH^+$ ($\lambda_{max}$=358 nm).

18) The $E^\circ_{ox}$ values were determined using the SHACV method (see Experimental Section), since the reported values in Ref. 8 were those obtained from irreversible peak potentials of the cyclic voltammograms by extrapolating to a scan speed at 0 mV $s^{-1}$. Thus, the $E^\circ_{ox}$ values determined in this study are somewhat larger than the reported values.

19) Eqs. 8, 9, and 10 are derived from Eqs. 3, 4, 5, 6, and 7, assuming that $[\mathbf{1}^{+•}]/[\mathbf{4}] \cong k_3[O_2]/k_1[\mathbf{1}]$, $[\mathbf{1}^{+•}]/[\mathbf{5}]=k_5/k_1$. The stoichiometry, $[\mathbf{1}^{+•}]+[\mathbf{4}]+[\mathbf{5}]=[AcrH^•]$ is also used to derive Eqs. 8, 9, and 10.

20) The first term in the right hand side of Eq. 8, which corresponds to the contribution of the non-chain process, may be neglected as compared to the second term for the radical chain process. Under the experimental conditions such that $k_6 \ll k_5$, $k_4[\mathbf{1}]/k_3[O_2] \gg k_2/k_1$, $\alpha$ is reduced to $\alpha \cong k_4k_5[\mathbf{1}]/(k_3[O_2])$, when Eq. 8 is reduced to Eq. 11.

21) The slight deviation from the linear correlation observed in Fig. 9 may be ascribed to the insufficiency for the conditions that $k_4[\mathbf{1}]/k_3[O_2] \gg k_2/k_1$, which is required for the linear correlation.